AWTEC 2012
Asian Wave and Tidal Conference Series
Nov. 27-30, Jeju Island, Korea

1st awtec 2012
Asian Wave and Tidal Energy Conference Series

Experimental Studies on the PTO System of a Novel Floating Wave Energy Converter

Mohammed Faizal[1], Byung-Ha Kim[1], Chang-Goo Kim[1], Nak-Joong Lee[1], M. Rafiuddin Ahmed[2], Young-Ho Lee[1#]

[1] Division of Mechanical & Energy System Engineering, College of Engineering, Korea Maritime University (KMU), 1 Dongsam-dong Youngdo-ku, Busan, 606-791, Korea
[2] Division of Mechanical Engineering, The University of the South Pacific, Suva, Fiji Islands.
Corresponding Author / E-mail: lyh@hhu.ac, TEL: +82-51-410-4293, FAX: +82-51-403-0381

KEYWORDS: wave energy; PTO system; cross flow turbine; novel wave energy converter

Experimental studies were carried out on the power-take off (PTO) system of a novel floating wave energy converter with a built-in cross-flow turbine. The pitching motion of the device causes a column of water to rise and fall periodically in a caisson which creates a bi-directional flow. The cross flow turbine uses this bi-directional flow to rotate in one direction only. The PTO system was experimented using a 6 DOF ocean simulator at a model to prototype scale of 1:3. The experiments were conducted for varying pitch angles, moment of inertia on shaft, wave periods, and rotational speeds. It was found that for all pitching angles, the device had optimum response at a wave period of 3 seconds. A moment of inertia of 0.053 kgm2 was found to be appropriate for all test cases. Peak hydraulic efficiencies between 35% - 45% were obtained for the range of 40 – 50 rpm for most test cases.

1. Introduction

A floating WEC utilizes the motion of the surface waves to generate electricity. The motions of a floating WEC are cyclic and there response depends on the frequency of the exciting waves. At wave frequencies corresponding to the natural frequency of the WEC, motions are more pronounced, and if suitably harvested, maximum power can be generated [1].

Power conversion or power take-off (PTO) systems are the main mechanisms that can be implemented to transfer energy from waves to the WEC, after which it gets converted to mechanical or electrical energy [2]. There are a large variety of wave energy conversion devices. The power conversion systems can however, be generalized into two main groups [3]: i) direct drive systems and ii) buffered systems. In a direct drive system, the PTO is the electrical generator. The moving part of a WEC is coupled directly to the moving part of an electrical generator, thus eliminating the need for intermediate mechanical devices such as turbines and hydraulic systems [4]. For buffered drive systems, the energy is captured and is transferred to a medium for temporary storage, after which it gets transferred to the generator. The storage acts as a buffer between the PTO stage and the generator in the power regulation stage [3]. Some of the most common buffered PTO systems are self-rectifying air turbines, hydraulic PTO systems, and high-pressure oil-hydraulics [5]

Model testing provides valuable information which can be used to predict how a prototype would behave under similar conditions [6]. Some principle benefits gained from model tests are validation of design values, obtain design empirical coefficients that can be directly applied to the prototype, verify the analytical techniques, verify offshore operation, and investigate unpredicted and unexpected phenomena [7]. The most appropriate scaling used for model tests of WEC's is the Froude scaling criteria. However, power representation in Froude scaling is very difficult due to the large power scaling factor between model and prototype. Offshore WEC model tests are mostly done at scales of 1:80 – 1:25 in small to medium sized wave tanks, and up to 1:10 scale in the largest and deepest wave tanks. Theses scales are extremely small for a PTO system to be realistically modelled and developed [8]. For example, for a scale of 1:10 and for a prototype PTO system of 100 kW, the model would have a power output of 0.03 kW, which is too small for a realistic simulation. The PTO mechanism can however be tested separately at a large model scale or at full scale by means of hydraulic or electrical actuators that directly drives the moving part of the PTO mechanism [8].

The present study focuses on the experimental studies of the PTO mechanism of a novel floating WEC with dimensions much smaller than the prevailing wavelength. The basic operation of the device is that it undergoes pitching motion caused by the waves, which in turn causes a column of water to rise and fall periodically in a caisson to create a bidirectional flow. This bidirectional flow drives a unidirectional crossflow turbine. The hydraulic performance of the Crossflow turbine is studied at various operating conditions.

2. The novel device

Fig. 1 shows a schematic of the novel device. This device uses the surface water displacement as an energy source. The pitching motion of

the device causes a column of water to rise and fall periodically in the double-hull housed in the caisson, creating a bi-directional flow. A cross-flow turbine uses this bi-directional flow to self-start and to rotate in one direction only. The working fluid inside the double-hull is fresh water. The cross-flow turbine does not have direct contact with sea water and is thus free from bio-fouling and is easy to maintain. A small opening to the atmosphere is provided to prevent pressure build up in the double-hull due to water motion. The power conversion system in this device is a buffered system, since a working fluid uses the wave energy to rotate a turbine, which then transfers energy to the generator.

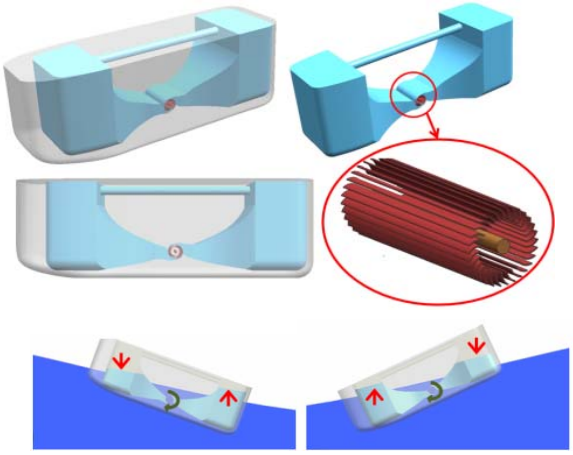

Fig. 1. A schematic diagram of the device.

Crossflow turbines are impulse turbines that are used for low head (<10 m) and medium head (10 – 50 m) applications [9]. In a cross-flow turbine, the water passes over the blades twice before exiting the turbine, resulting in a higher momentum transfer [10]. Some advantages and characteristics of the cross-flow turbine are that a wide range of rotational speeds can be selected, the turbine diameter does not depend on the flow rate, satisfactory efficiency levels, and are simple to manufacture.

Several studies have been carried out on crossflow turbines. Choi et al. [11] did a performance study and assessed the internal flow characteristics of a Crossflow hydro turbine by varying the shapes of the nozzle and the runner blades. They concluded that pressure and velocity in the flow passage change with changing nozzle shape, runner blade angle and number of blades. Prasad et al. [12] presented numerical studies on the effects of front guide nozzle shape on the flow characteristics of an augmentation channel for a Crossflow turbine used for wave energy conversion. Three different guide nozzles were studied. They studied how the front guide nozzle shape influences the flow downstream in the augmentation channel, water power in the channel, and the first stage energy conversion efficiencies.

Choi et al. [13] carried out an experimental investigation on the effects of wave conditions on the performance of a Crossflow turbine for wave energy conversion in a reciprocating flow. The results showed that the rotational speeds, turbine differential pressure, maximum power output and best turbine efficiencies vary a lot with various wave conditions. Choi et al. [14] and Lee et al. [15] presented numerical and experimental results on the performance of a Crossflow turbine used in a reciprocating flow for wave energy conversion. The internal flow was observed using CFD. A turbine efficiency of 48.6% was achieved under wave conditions for a reciprocating flow in a 2D wave channel. They concluded that large vortex and circulations could consume a lot of the output power.

The cyclic motion of the partly filled working fluid (fresh water) in the caisson is being studied by many researchers as a sloshing phenomenon. Sloshing is the liquid motion in partially filled liquid tanks due to the frequency of tank oscillation being close to natural frequency of liquid in water tank. Large sloshing amplitudes are expected when the frequency of the tank motion is close to the natural frequency of the liquid inside. The motion of the sloshing liquid depends on the type of disturbance/excitation causing it [39]. Several studies have been carried out on sloshing of liquids in excited tanks.

Akyildiz and Ünal [16] performed an experimental investigation on the pressure distribution at different locations and 3D effects of liquid sloshing on a rectangular tank. Mitra et al. [17] presented simulation results of a 3D fully coupled analysis of nonlinear sloshing and ship motion. They investigated the coupling effects of six degrees of freedom in ship motion with fluid motion inside a 3D tank. The sloshing effect was investigated for several factors such as container parameters, significant wave height, current and wind velocities, and wave and current effects on the ship. Marsh et al. [18, 19] studied sloshing as an absorber for structural control. Kyoung et al. [20] simulated a numerical nonlinear sloshing problem for impact loading on the tank structure. The wave impact load on the structure was obtained numerically for a nonlinear free surface condition and compared with the predictions made using Morison's formula. Chen and Chiang [21] presented a 2D numerical analysis of sea wave induced fully nonlinear sloshing fluid in a rigid floating tank. The interaction effect between the fully nonlinear sloshing liquid and the floating tank associated with coupled surge, heave, and pitch motion of the tank were studied.

Wu and Chen [22] presented studies on sloshing waves and resonance modes of fluid motion in a 3D tank by a time-independent finite difference method. They studied a range of excitation frequencies with motions that exhibit multiple degrees of freedom.

The use of the cyclic motion of the partly filled water in a tank like structure to drive a crossflow turbine to convert wave energy to generate electricity has never been reported before. This device has advantages such as the working fluid that drives the turbine is fresh water, therefore, no corrosion and bio-fouling of the turbine from ocean water. It is compact and free from aerodynamic noises of high speed turbines, and can be much easily installed into arrays in a wave farm.

3. Experimental procedure

The PTO system was tested using a Sunsystem 6 DOF ocean

simulator with a capacity of 5 Tonnes. The maximum angle for pitch in the system is ±10° with a resolution of ± 0.1°. The maximum length for heave in the system is ±0.5m with a resolution of ±0.1m. The range of frequencies in the system is 0.1 – 0.5Hz. The experiments were conducted at a model to prototype scale of 1:3. Fig. 2 shows the geometric details of the double-hull of the device.

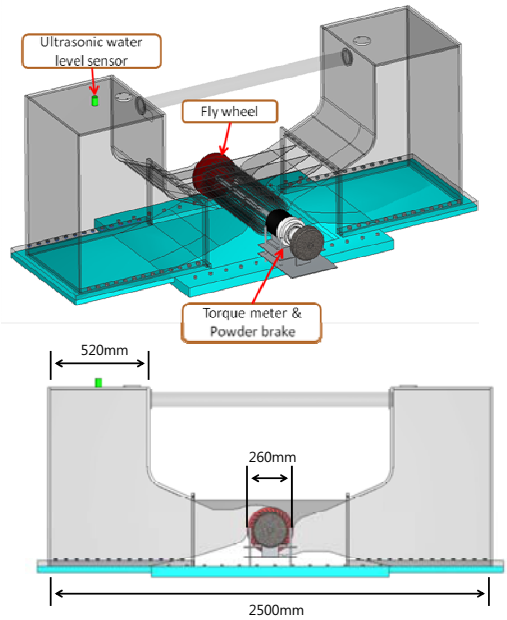

Fig. 2. Geometric details of the double-hull of the device

.

Fig. 3 shows the geometric details of the crossflow turbine and the augmentation channel. For a given flow direction, the augmentation channel served as a nozzle at the inlet side and as a diffuser at the exit side. There are a total number of 30 blades used. The outer diameter of the turbine is 250 mm, where as the internal diameter is 240 mm. The flow through the turbine is radial and the water passes over the blades twice before exiting the turbine. The blades make an angle of 30º to the tangent at the outer periphery and an angle of 90º to the tangent at the inner periphery. The clearance of the turbine and housing is 20.6 mm.

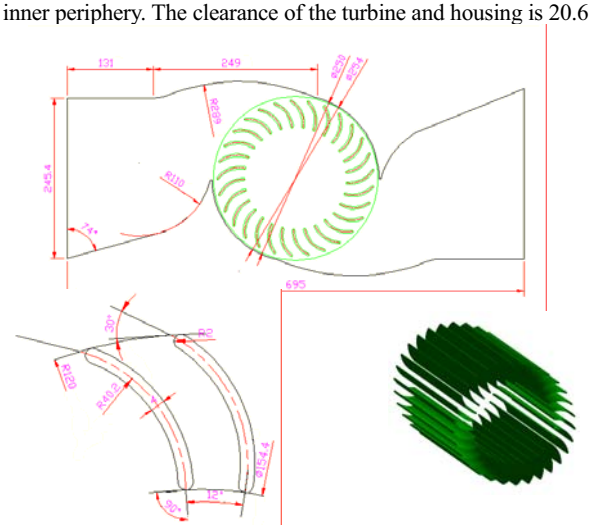

Fig. 3. Geometric details of the crossflow turbine and the augmentation channel (dimensions in mm).

A General Acoustics UltraLab® ULS sensor, (model USS20130) with a resolution of 0.36 mm, measuring range of 200 – 1300 mm, and a measurement frequency of 200 kHz was mounted on the left tank to record the change in water level. This change in water level was used to calculate the flowrate of the water (or the working fluid) in the double-hull at different operating conditions. Two pressure holes on the sidewalls, before and after the turbine, were used to measure the pressure drop across the turbine. A Sensys pressure transducer (model DWSD0020R1AA) with a pressure range of 0 – 20kPa and accuracy of 0.075% was used to measure the differential pressure of the turbine.

A SETech torque transducer-RPM type (model YDR – 5KM) with a capacity of 49.03 Nm and maximum rpm of 6000 was used to record the torque and rotational speeds. A Pora powder brake (model PRB-Y3) with a torque rating of 3 Nm was used to control the torque and thus the rotational speed of the turbine. A flywheel with a mass of 4 kg is attached to the shaft of the turbine to ensure that there is continuous rotation throughout a given cycle. All the digital signals from the sensors are acquired on a Graphtec GL500A data logger (model GL500-UM-852). The sampling interval of all the data was set to 1ms.

Experiments were first carried out without any load on the shaft to determine the maximum rotational speed for all cases. The pitching angle was varied from 2 – 10° in increments of 2°, and the range of pitching frequencies tested were between 0.25 – 0.5 Hz, while the water level in the double-hull was kept constant at 550 mm. The with load conditions were tested for a frequency of 0.33 Hz and 0.5 Hz, and a rotational speed range of 10 – 80 RPM. Repeat tests on a few selected loaded cases give measurement uncertainties as: Q = ± 1.5 percent, ΔH = ± 1.0 percent, T = ± 1.2%. Fig. 4 shows a picture of the device on the ocean simulator.

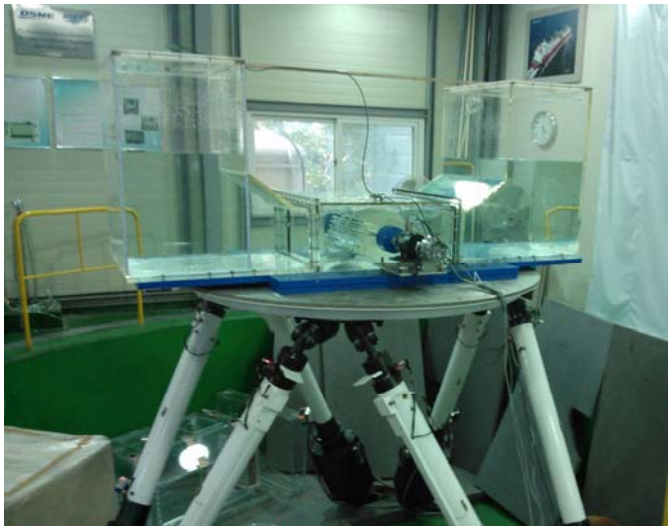

Fig. 4. Picture of the device on the ocean simulator.

4. Results and discussion

Fig. 5 shows the turbine rotational speed, N, and the flowrate, Q, of water in the double-hull against the pitching angle, θ, at three different wave periods, T, for a no-load condition. Initial experiments were performed without any loads on the shaft to determine the maximum rotational speeds at various conditions.

For a given T, both Q and N increase with increasing θ. For a given T and with increasing θ, the potential energy of the water in the hull increases due to higher inclination, therefore, the change in water level is more, and thus Q and N increases. The potential energy of the water gets converted to kinetic energy as the water travels from one hull to the other. A maximum N of 108.663 RPM was obtained for T = 3 s and θ = 10°.

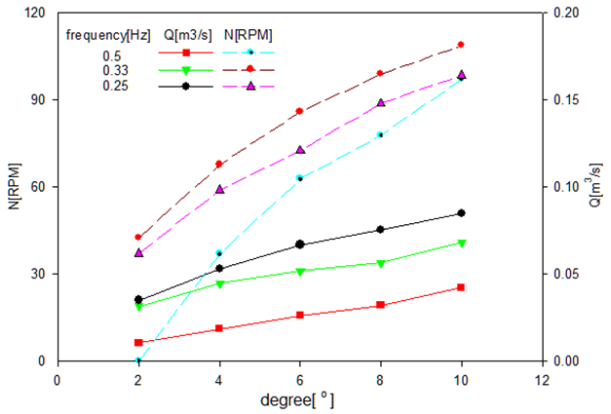

Fig. 5. The rotational speed, N, and flowrate, Q, at different pitching angles, θ.

Fig. 6 shows N and Q against varying T, for four different θ, for a no-load condition. For a given θ, and increasing T, N increases and gets to a peak at T = 3 s, after which it begins to decrease. For all test cases, bubbles and circulation were observed only for T = 3 seconds. The higher N and the chaotic motion of the water at T = 3 s is observed due to the natural frequency of oscillation being close to the natural frequency of the device [10, 39].

The flowrate, Q, increased with increasing T for all θ. Sloshing at the free surface of water in the double-hull was observed at higher angles, but the chaotic motion (bubbles and circulation) of the water was only observed for T = 3 s, for all cases.

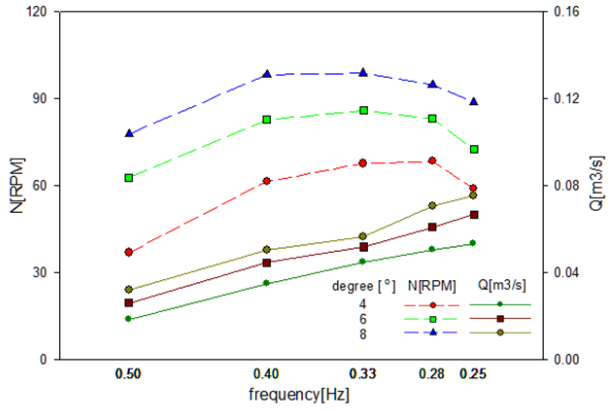

Fig. 6. Rotational speed, N, and flowrate, Q, at different wave periods, T.

The results of the no-load condition tests were used to design the loaded condition tests. The N values of the turbine at different operating conditions were used to decide the N values of the Powder Brake. The load condition tests were focussed on T = 3 s since maximum N is obtained for this period for all cases. Loaded tests were also carried out for T = 2 s (the lowest period) to compare the performance. Figure 7a and Fig 7b shows the flywheel tests at 40 RPM and 0.33 Hz and 0.25 Hz. For T = 3 s, efficiency increases with increasing flywheel mass. For T = 2 s, the peak efficiency is observed at 8 kg mass. The efficiency gap is small for T = 3 s.

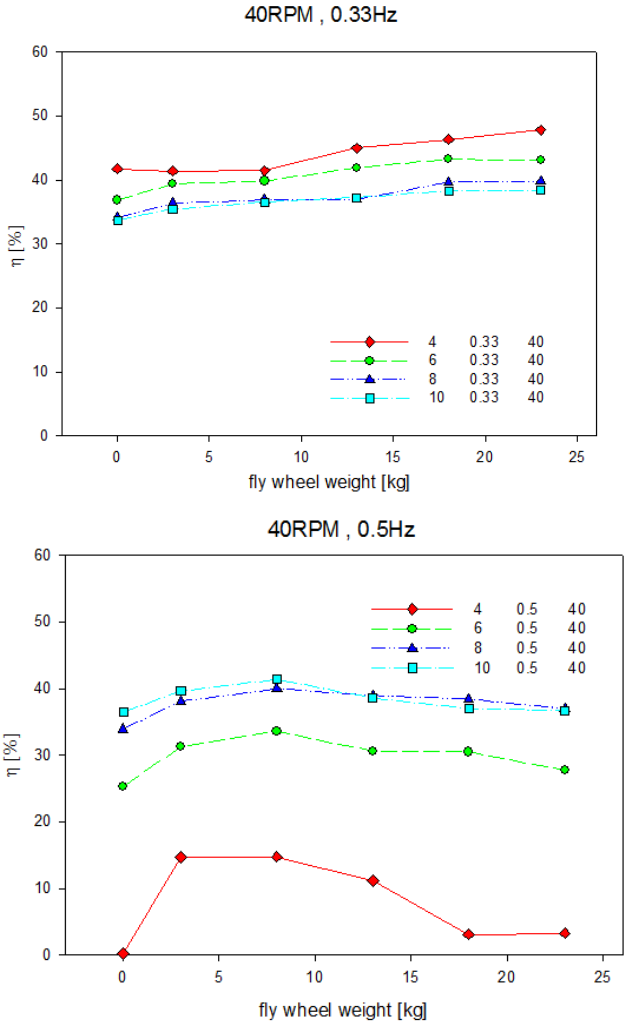

Fig. 7. Hydraulic efficiency, η, against flywheel weight for N = 40 RPM and for a) T = 3 s b) T = 2 s

Figure 8a and 8b shows the flywheel tests at 50 RPM and 0.33 Hz

and 0.25 Hz. For T = 3s, efficiency increases with increasing flywheel mass. For T = 2s, efficiency reduces after 8 kg flywheel mass. The 8 kg mass is therefore chosen, to have favourable efficiencies

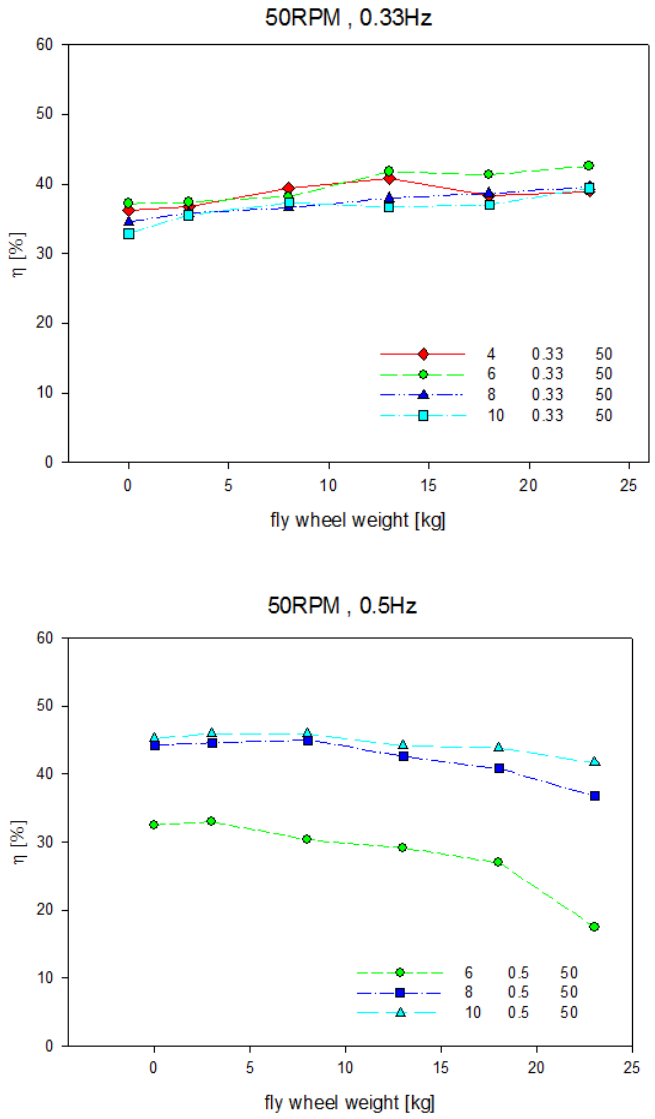

Fig. 8. Hydraulic efficiency, η, against flywheel weight for N = 50 RPM and for a) T = 3 s b) T = 2 s

Figure 9a and Figure 9b shows the hydraulic efficiency, η, against N for T = 3 s and T = 2 s, for varying θ. For T = 3 s, a maximum η of 45% is obtained at θ = 4° and N = 30 RPM. For T = 2 s, a maximum η of 45% is obtained at θ = 10° and N = 50 RPM. The design rotational speed, N, for this device can be considered to be between 40 – 50 RPM, since for T = 3s, the range of efficiencies is between 35% to 45%. For all θ values and for a given corresponding N, the difference between η for T = 2 s is more compared to T = 3 s.

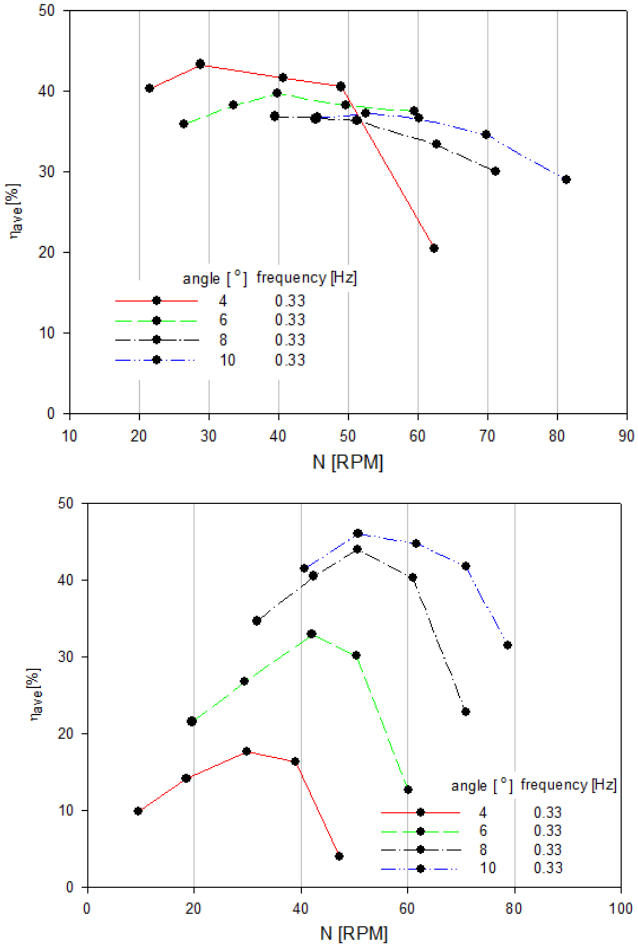

Fig. 9. Hydraulic efficiency against N for varying angles a) T = 3 s b) T = 2 s

Fig. 10 shows the results for heaving. It can be seen that the efficiencies and the power output is almost constant for al heaving ranges. Therefore it can be said that heaving does not really affect the performance.

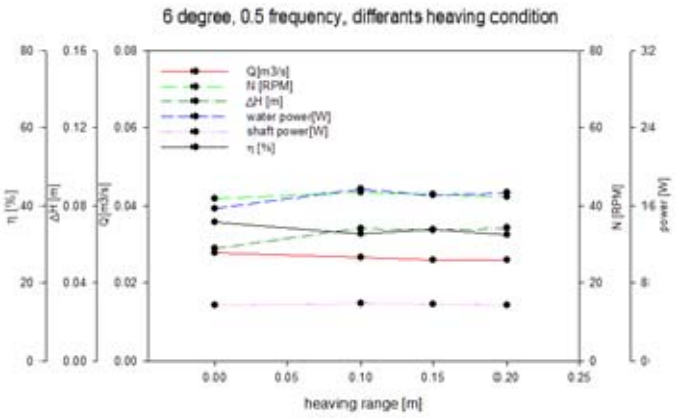

Fig. 10. Performance characteristics at varying heaving range.

5. Conclusions

Experimental studies were carried out on PTO system of a novel floating wave energy converter with a built-in cross-flow turbine at a scale of 1:3.. Higher performance is achieved at a period of 3 seconds. The design rotational speed of this device can be considered between 40 – 50 RPM. A 8 kg flywheel was found to be appropriate for all operating conditions. Peak hydraulic efficiencies between 35% - 45% were obtained for the range of 40 – 50 rpm for most test cases

Acknowledgements

This work is the outcome of a Manpower Development Program for Marine Energy by the Ministry of Land, Transport and Maritime Affairs (MLTM) and New & Renewable Energy R&D program (2011T100100688) under the Ministry of Knowledge Economy, Republic of Korea.

References

1. [Payne GS, Taylor JRM, Bruce T, Parkin P. Assessment of boundary-element method for modelling a free-floating sloped wave energy device. Part 1: Numerical modelling. Ocean Engineering 2008; 35(3-4): 333-341.
2. Thomas G. The Theory Behind the Conversion of Ocean Wave Energy: A Review, in: Cruz J (Ed.), Ocean wave energy: current status and future perspectives. Heidelberg: Springer; 2008: 41-91.
3. Price AAE. New Perspectives on Wave Energy Converter Control. PhD thesis: The University of Edinburgh; 2009
4. Baker NJ, Mueller MA. Direct Drive Wave Energy Converters. Rev. Energ. Ren. : Power Engineering 2001; 1-7. Available online at: http://www.cder.dz/download/upec-1.pdf
5. Falcão AF de O. Wave energy utilization: a review of technologies. Renewable and Sustainable Energy Reviews 2010;14(3):899-918.
6. Chakrabarti SK. The theory and practice of hydrodynamics and vibration. Singapore: World Scientific Publishing Co. Pte. Ltd; 2002.
7. Chakrabarti SK. The theory and practice of hydrodynamics and vibration. Singapore: World Scientific Publishing Co. Pte. Ltd; 2002.
8. Falcão AF de O, Pereira PER, Henriques JCC, Gato LMC. Hydrodynamic simulation of a floating wave energy converter by a U-tube rig for power take-off testing. Ocean Engineering 2010; 37(14-15): 1253-1260
9. Paish O. Small hydro power: technology and current status. Renewable and Sustainable Energy Reviews 2002; 6(6):537-556.
10. Babarit A, Clément AH, Gilloteaux JC. Optimization and time-domain simulation of the SEAREV wave energy converter, paper no. OMAE2005-67286. In: Proceedings of the ASME 24th International Conference on Offshore Mechanics and Arctic Engineering, Halkidiki, Greece: 2005.
11. Choi YD, Lim JI, Kim YT, Lee YH. Performance and internal flow characteristics of a Cross-flow hydro turbine by the shapes of nozzle and runner blade. Journal of Fluid Science and Technology 2008;3(3):398-409.
12. Prasad D, Zullah MA, Ahmed MR, Lee YH. Effect of front guide nozzle shape on the flow characteristics in an augmentation channel of a direct drive turbine for wave power generation. Science China: Technological Sciences 2010;53(1):46-51.
13. Choi YD, Kim CG, Lee YH. Effect of wave conditions on the performance and internal flow of a direct drive turbine. Journal of Mechanical Science and Technology 2009; 23:1693-1701.
14. Choi YD, Kim CG, Kim YT, Song JI, Lee YH. A performance study on a direct drive hydro turbine for wave energy converter. Journal of Mechanical Science and Technology 2010; 24(11):1-10.
15. Lee YH, Kim CG, Choi YD, Kim IS, Hwang YC. Performance of a direct drive hydro turbine for wave power generation. IOP Conf. Series: Earth and Environmental Science 25th IAHR Symposium on Hydraulic Machinery and Systems 2010; 12-012029.
16. Akyildiz H, Ünal E. Experimental investigation of pressure distribution on a rectangular tank due to the liquid sloshing. Ocean Engineering 2005; 32(11-12): 1503-1516.
17. Mitra S, Wang CZ, Reddy JN, Khoo BC. A 3D fully coupled analysis of nonlinear sloshing and ship motion. Ocean Engineering 2012; 39: 1-13.
18. Marsh A, Prakash M, Semercigil E, Turan ÖF. A shallow-depth sloshing absorber for structural control. Journal of Fluids and Structures 2010; 26(5): 780-792.
19. Marsh A, Prakash M, Semercigil E, Turan ÖF. A study of sloshing absorber geometry for structural control with SPH. Journal of Fluids and Structures 2011; 27(8): 1165-1181.
20. Kyoung JH, Hong SY, Kim JW, Bai KJ. Finite-element computation

of wave impact load due to a violent sloshing. Ocean Engineering 2005; 32(17-18): 2020-2039.

21. Chen BF, Chiang HW. Complete two-dimensional analysis of sea-wave-induced fully non-linear sloshing fluid in a rigid floating tank. Ocean Engineering 2000; 27(9):953-977.

22. Wu CH, Chen BF. Sloshing waves resonance modes of fluid in a 3D tank by a time-independent finite difference method. Ocean Engineering 2009;36(6-7): 500-510.